JOURNAL OF OPTOELECTRONICS AND ADVANCED MATERIALS, Vol. 9, No. 10, October 2007, p. 3247 - 3252

Atomic- and void-species nanostructures in chalcogenide glasses modified by high-energy γ-irradiation

T. KAVETSKYY[a-c], O. SHPOTYUK[a,c*], I. KABAN[b], W. HOYER[b]
[a]*Institute of Materials, Scientific Research Company "Carat", 202 Stryjska Str., 79031 Lviv, Ukraine*
[b]*Institute of Physics, Chemnitz University of Technology, D-09107 Chemnitz, Germany*
[c]*Institute of Physics, Jan Dlugosz University, Al. Armii Krajowej 13/15, Czestochowa 42201, Poland*

Atomic- and void-species nanostructures are studied in As_2S_3 glass in unmodified and γ-modified states using a combination of conventional X-ray diffraction in respect to the first sharp diffraction peak, synchrotron-based high-energy X-ray diffraction and extended X-ray absorption fine structure spectroscopy. The experimental data are analyzed taking into account radiation-induced changes in the parameters of the first sharp diffraction peak (position, full width at half maximum, intensity), packing factor, structural disordering, atomic and void topology, coordination number and mean square deviation in bond length. The origin of the structural modification effect induced by γ-irradiation is explained in terms of coordination topological defects model.

(Received July 3, 2007; accepted October 1, 2007)

Keywords: Chalcogenide glasses, Nanostructure, First sharp diffraction peak, Nanovoids, Radiation modification

1. Introduction

An adequate understanding of structure-properties correlation in chalcogenide glasses, one of the most promising optoelectronic materials, is of a high interest for scientists and numerous well-known electronic firms from all over the world. The atomic-species nanostructure is typically taken as the main determinant for physical-chemical properties and exploitation possibilities of these glasses, but the knowledge of the atomic distribution alone is not always enough for this. No more important information can also be obtained from void-species nanostructure of glasses – the internal structural nanovoids frozen near glass transition.

The present work is aimed to study atomic- and void-species nanostructures in the most typical representatives of chalcogenide glasses, the vitreous arsenic trisulfide As_2S_3, using known diffraction techniques such as conventional X-ray diffraction in respect to the first sharp diffraction peak (FSDP-related XRD), synchrotron-based high-energy X-ray diffraction (HEXRD) and extended X-ray absorption fine structure (EXAFS) spectroscopy.

2. Experimental

The experimental measurements were carried out for unmodified and structurally-modified samples of As_2S_3 glass (g-As_2S_3) prepared by conventional melt-quenching procedure [1]. Before experiment, the disk-like samples were polished to ~1.5 mm in thickness with high optical quality and annealed at ~25 K below glass transition temperature (T_g = 456 K) [2].

The ^{60}Co γ-irradiation (typical example of high-energy photon flux treatment) was used as structure modification factor, which is characterized by significant preferences among different types of ionizing irradiation [3]: (i) the average energy of ^{60}Co γ-quanta (1.25 MeV) is greater than the dual rest energies of electrons (1.02 MeV); (ii) the γ-irradiation is characterized by a high penetration ability and, consequently, a high uniformity of the produced structural changes throughout a sample; (iii) the γ-irradiation does not cause direct atomic displacements resulting in surface macro-damages, craters or cracks, proper to high-energy corpuscular radiation (accelerated electrons, protons, neutrons); (iv) the nuclear transmutations, induced by reactor neutrons and essentially constraining experimental possibilities for radiation-induced effects observation, do not take place during γ-irradiation. The radiation treatment of the investigated samples was performed at the normal conditions of stationary radiation field, created in a closed cylindrical cavity by a number of concentrically established ^{60}Co radioisotope capsules. The accumulated dose of Φ = 2.41 MGy was chosen with account of the previous results [4,5]. No special measures were taken to prevent the uncontrolled thermal annealing of the samples, but maximum temperature in the irradiating camera did not exceed 320-330 K during prolonged γ-irradiation (more than 10 days), providing absorbed dose power $P < 5$ Gy/s.

The conventional FSDP-related XRD study was carried out using HZG-4a diffractometer (Cu K_α-radiation). Diffraction data were collected in the range of $10 \le 2\theta \le 30°$ (a step of 0.05° and an integration time of 70 s/point). The samples were measured in the "rotation" regime (2 revolutions per second). The FSDP position 2θ was determined with an accuracy of ±0.1°.

The HEXRD experiments were carried out at the synchrotron experimental station BW5 at HASYLAB,

DESY in Hamburg, Germany. The investigated samples were examined in transmission geometry. The energy of radiation was 98.9 keV (0.125 Å). The scattered intensity was measured between 0.5 and 18 $Å^{-1}$, the raw data being corrected for detector dead-time, polarization, absorption and variations in detector solid angle [6]. After correction of the raw data, the scattering intensity measured in arbitrary units was converted into the coherent scattering intensity per atom in electronic units using a generalized Krogh-Moe-Norman method [7,8]. The Compton scattering was also corrected using the values given by Cromer and Mann [9]. Then, the Faber-Ziman [10] total structure factor $S(Q)$ was calculated from scattering intensity as

$$S(Q) = \frac{I_{\text{e.u.}}^{\text{coh}}(Q)}{\langle f^2(Q)\rangle}, \quad (1)$$

with

$$\langle f^2(Q)\rangle = \sum_i c_i f_i^2(Q), \quad (2)$$

where c_i is molar fraction and $f_i(Q)$ is total scattering atomic factor of the i-th component of the glass.
The total pair distribution function $g(r)$ was obtained via transformation

$$g(r) = \frac{\rho(r)}{\rho_0} = 1 + \frac{1}{2\pi^2 r\rho_0}\int_0^\infty Q[S(Q)-1]\sin(Qr)\mathrm{d}Q, \quad (3)$$

where $\rho(r)$ and ρ_0 are local and average number density, respectively.

The position of the first maximum of $g(r)$ is the mean nearest-neighbour distance r. The coordination number calculated as

$$N = \int_{r1}^{r2} 4\pi r^2 \rho_0 g(r)\mathrm{d}r, \quad (4)$$

is mean number of nearest neighbours in respect to the chosen atom, while r_1 and r_2 denote the lower and upper limits of the first maximum in the radial distribution function $4\pi r^2\rho(r)$.

The EXAFS experiments at As K-edge were carried out at the synchrotron beam line X (HASYLAB) in transmission mode using Si (111) double-crystal monochromator. The pieces of glassy As_2S_3 were finely ground, mixed with cellulose and pressed into tablets. The EXAFS intensities were measured by ionization chambers filled with Kr. The sample quantity in the tablets was adjusted to the composition of the sample and to the selected edge. The EXAFS spectra were obtained with 0.5 eV step in a vicinity of absorption edge. The measuring time was k-weighted during collection of the signal, the standard programmes ATHENA and ARTEMIS being used for data processing.

3. Results

Fig. 1 shows FSDP-related XRD patterns for g-As_2S_3 in the initial and γ-irradiated states. The FSDP parameters obtained are presented in Table 1. It is noteworthy that practically no radiation-induced effect on the FSDP position $2\theta_{\text{FSDP}}$ is observed, while the FSDP full width at half maximum (FWHM) β_{FSDP} is strongly modified after irradiation.

Following the well-known Scherrer's approach based on FSDP data (position and FWHM) [11,12], the average thickness of the domain built by packing of disordered layers D_S and interlayer distance d_S can be estimated as:

$$D_S = (K\lambda/\beta_{\text{FSDP}}\cos\Theta_{\text{FSDP}})\cdot(360/2\pi), \quad (5)$$

and

$$d_S = \lambda/2\sin\Theta_{\text{FSDP}}, \quad (6)$$

where K = 0.9 is Debye-Scherrer constant, λ is X-ray wavelength.

The ratio between D_S and d_S

$$p = D_S/d_S, \quad (7)$$

is the so-called "packing" factor which can be considered as a measure of the layer packing in an amorphous domain.

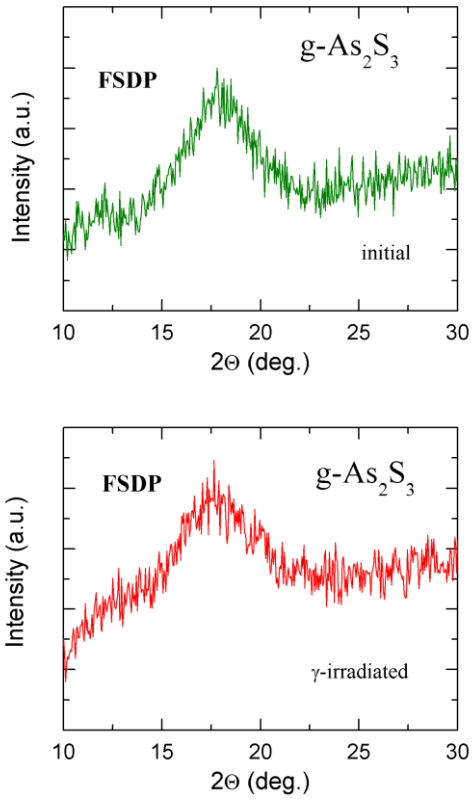

Fig. 1. The FSDP-related XRD patterns (Cu K_α-radiation) for g-As_2S_3 in the initial and γ-irradiated states.

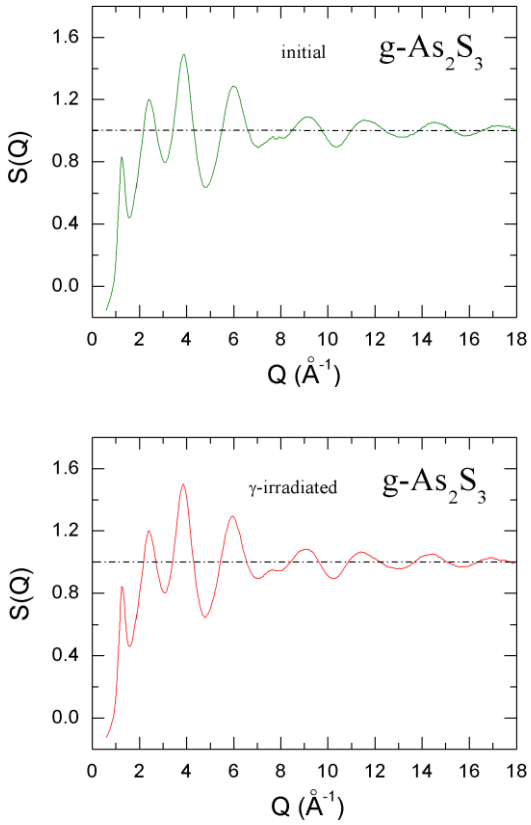

Fig. 2. The experimental structure factors S(Q) obtained from HEXRD measurements for g-As_2S_3 in the initial and γ-irradiated states.

Table 1. The FSDP-related data for g-As_2S_3 in the initial and γ-irradiated states obtained using conventional XRD technique. $2\Theta_{FSDP}$ is the FSDP position, β_{FSDP} is the FWHM of the FSDP, D_S is the average thickness of the domain built by disordered layers, d_S is the interlayer distance, p is the "packing" factor.

Glass As_2S_3	$2\Theta_{FSDP}$ (deg.)	β_{FSDP} (deg.)	D_S (Å)	d_S (Å)	$p = D_S/d_S$
initial	17.8 ± 0.1	3.9 ± 0.1	20.6 ± 0.1	5.0 ± 0.1	4.12
γ-irradiated	17.6 ± 0.1	4.4 ± 0.1	18.3 ± 0.1	5.0 ± 0.1	3.66

One can see that decrease in the packing of amorphous layers after irradiation is caused by reduction of the average thickness of the domain and, hence, the sizes of the ordered domains decrease.

Fig. 2 shows the experimental structure factors $S(Q)$ obtained by HEXRD for g-As_2S_3 in the initial and γ-irradiated states. The parts of the $S(Q)$ in the FSDP region and the structure factor difference $\Delta S(Q)$ induced with γ-irradiation are illustrated in Fig. 3. There is no change in the FSDP position (Q_{FSDP} = 1.25 ± 0.05 Å^{-1}), while the FSDP intensity decreases after γ-irradiation.

Fig. 4 demonstrates the pair distribution functions $g(r)$ for g-As_2S_3 in the investigated states. The values for the first- and second nearest neighbour distances r_1 and r_2 are found to be within the range of 2.27-2.30 Å and 3.48-3.50 Å (Table 2), respectively, in a good agreement with known reference data [13,14]. The mean nearest-neighbour distances are practically not changeable after irradiation (this is also confirmed by the EXAFS data presented below). At the same time, the intensity $g(r_1)$ for first coordination shell significantly decreases after irradiation, while the intensity $g(r_2)$ for second shell remains practically the same. The first coordination number N obtained using Eq. (4) is found to be slightly increased with irradiation from 2.46 to 2.58.

The EXAFS As K-edge $\chi(k)k^3$ spectra for g-As_2S_3 in the initial and γ-irradiated states and their Fourier-transforms are shown in Fig. 5. The corresponding fitted values of EXAFS parameters (the mean nearest neighbour distance r_1, mean square deviation in bond length or Debye-Waller factor σ^2 and partial coordination number N_e of As or number of As atoms surrounding As) are gathered in Table 3.

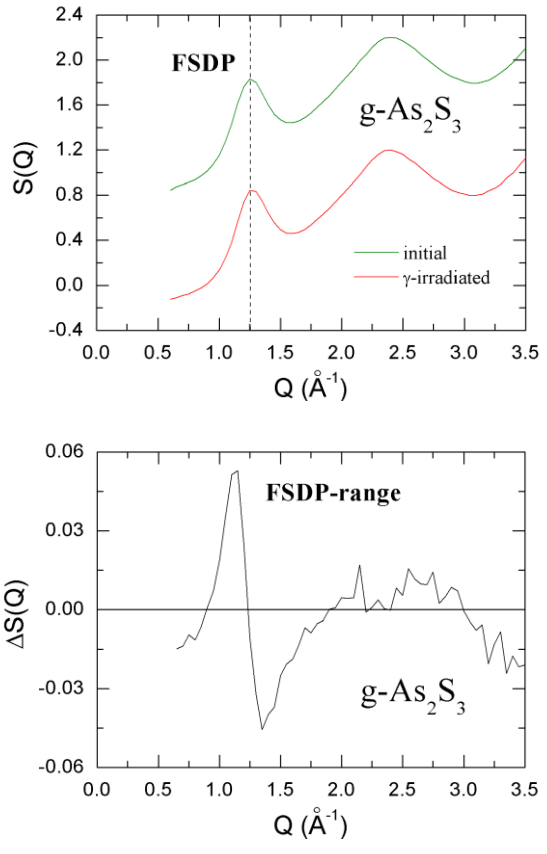

Fig. 3. The experimental structure factors S(Q) for g-As_2S_3 in the initial and γ-irradiated states in the FSDP region (the curve for initial state is shifted for clarity) and the structure factor difference ΔS(Q) induced with γ-irradiation (positive difference means intensity decrease with γ-irradiation).

Table 2.The first and the second nearest neighbour distances r_1 and r_2, the pair distribution function intensities $g(r_1)$ and $g(r_2)$, and the first coordination number N for g-As_2S_3 in the initial and γ-irradiated states obtained using HEXRD technique.

Glass As_2S_3	r_1 (Å)	$g(r_1)$	r_2 (Å)	$g(r_2)$	N
initial	2.27 ± 0.05	4.74	3.48 ± 0.05	2.28	2.46 ± 0.13
γ-irradiated	2.30 ± 0.05	4.09	3.50 ± 0.05	2.25	2.58 ± 0.13

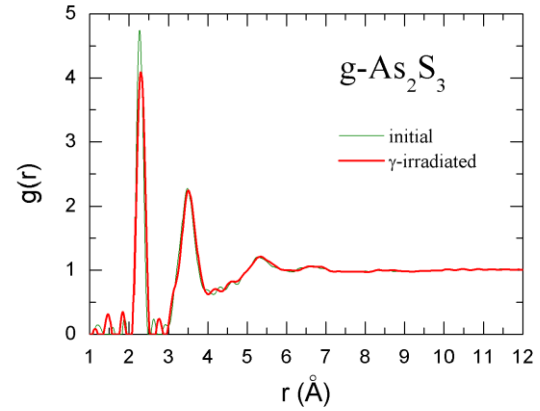

Fig.4. The pair distribution functions g(r) for g-As_2S_3 in the initial and γ-irradiated states.

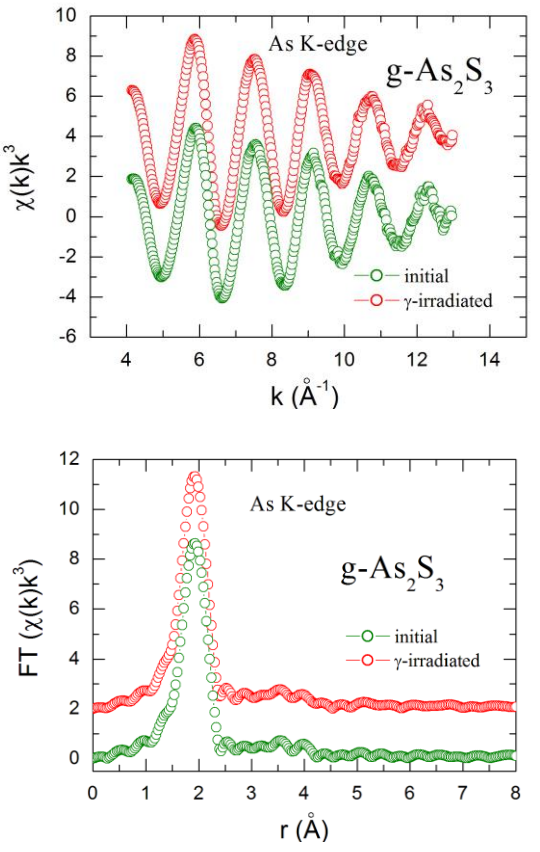

Fig. 5. The EXAFS As K-edge $\chi(k)k^3$ spectra and their Fourier-transforms (without phase shift correction) for g-As_2S_3 in the initial and γ-irradiated states. The curves for γ-irradiated sample are shifted for clarity.

Table 3.The fitted values of the mean neighbour distance r_1, the mean square deviation in bond length σ^2, and the partial coordination number N_e of As obtained from As K-edge EXAFS spectra for g-As_2S_3 in the initial and γ-irradiated states.

Glass As_2S_3	r_1 (Å)	σ^2 (× 10^{-4} Å^2)	N_e
initial	2.28 ± 0.01	40 ± 0.5	2.44 ± 0.20
γ-irradiated	2.28 ± 0.01	43 ± 0.5	2.92 ± 0.20

4. Discussion

Recently Kavetskyy and Shpotyuk [15] have shown that the XRD patterns treated within Elliott's void-based model for the FSDP [16,17] along with positron annihilation lifetime spectroscopy (PALS) is useful experimental tool to examine interstitial nanovoids in topologically disordered materials. It has been established, in part, that for chalcogenide glasses like to arsenic selenide g-As_2Se_3, the FSDP position Q_{FSDP} and nanovoid diameter D_v are linked through expression [15]:

$$Q_{\mathrm{FSDP}} = 2.3\pi / D_{\mathrm{v}}. \quad (8)$$

Assuming from PALS results [18] the same nanovoids can be responsible for the FSDP occurrence in both arsenic selenide and sulphide, the Eq. (8) established for g-As_2Se_3 seems to be also applicable for g-As_2S_3. The volume of interstitial nanovoids for the unmodified g-As_2S_3 estimated with Eq. (8) is found to be equal 97 ± 5 Å^3 (2.85 ± 0.1 Å in radius). This corresponds to the volume of about three atomic vacancies.

It should be noted that existence of nanovoids with the radius of ~2.9 Å was also predicted in chalcogenide glasses theoretically using Monte-Carlo modeling procedure [19]. Such size of nanovoids for g-As_2S_3 is in a good agreement with the results for g-As_2Se_3 obtained by Monte-Carlo simulation [20], PALS [18], and FSDP-related XRD and PALS [15]. It means that void-species nanostructure of the binary chalcogenide glasses based on arsenic-containing $AsX_{3/2}$ pyramids can naturally be determined by the cation-cation correlations like to Elliott's void-based model for the FSDP in the case of AX_2-type non-crystalline materials in which the FSDP is a chemical-order prepeak in the total structure factor $S(Q)$ due to ordering of interstitial voids around cation-centred structural units [16,17]. The similar conclusion has been made for glassy and liquid As_2Se_3 studied by anomalous X-ray scattering [21].

High-energy γ-irradiation leads to some changes in the FSDP intensity and FWHM, but practically does not affect the FSDP position (see Table 1 and Fig. 3). The latter means, in terms of Eq. (8), that the size of nanovoids is not modified by irradiation, while the former probably indicates effect of γ-irradiation on nanovoid distribution in a glass network (e.g., creation or annihilation of nanovoids, rearrangements of nanovoids due to structural transformations, etc.).

The radiation-induced FSDP changes observed well correlate with light-induced changes for As_2S_3 glass

reported by Tanaka [22]. So after illumination of g-As_2S_3 the angular shifts of the FSDP position were also not detected or very small, and the peak became weaker and broader. The FSDP position for g-As_2S_3 found by Tanaka [22] (1.2 Å^{-1}) well agrees with the value detected in the present study (1.25 ± 0.05 Å^{-1}). Hence, interlayer distance $R = 2\pi/Q_{FSDP} \approx 5.2$ Å, representing the FSDP, also correlates with our results.

In order to analyze γ-irradiation effect on nanovoid distribution, the proportionality between macroscopic volume change $\Delta V/V$ and $\Delta R/R$ (where ΔR is considered as local changes in the interlayer separation) should be taken into account. In this approach the magnitude of $\Delta R/R$ can be estimated using the expression like to one reported in [22]:

$$\Delta R/R \cong -\int Q\,\Delta S(Q)\,dQ \,/\, \int Q\,S(Q)\,dQ, \qquad (9)$$

where $S(Q)$ is the structure factor in the FSDP region in the initial state, and $\Delta S(Q)$ is the radiation-induced change. According to Tanaka [22], the integration should be performed over the FSDP (0.5 - 2 Å^{-1}). The value of $\Delta R/R$ in our case is found to be equal 1 ± 0.5 % in a good agreement with Tanaka's results.

Table 4 summarizes radiation-induced changes in atomic- and void-species nanostructures obtained by XRD and EXAFS techniques for g-As_2S_3. The EXAFS data for amorphous a-Se taken from Ref. [23] are given in the table for comparison.

Table 4. Radiation-induced changes in the XRD and EXAFS data for g-As_2S_3.

Method	Excitation	FSDP position	FSDP intensity	FWHM	$\Delta R/R$ (%)	$\Delta V/V$ (%)
XRD	light	not detected [a]	reduction [a]	broader [a]	+ 1 ± 0.5 [a] *	+ 0.4 [a] **
	γ-ray	not detected [b]	reduction [b]	broader [b]	+ 1 ± 0.5 [b]	–
Method	Excitation	Bond distance	Debye-Waller factor		Coordination number	
EXAFS	light (for a-Se)	not detected [c]	increase [c]		increase [c]	
	γ-ray	not detected [b]	increase [b]		increase [b]	

[a] Reference [22];
* The value obtained by XRD method;
** The value in the volume changes (photoexpansion) reported in [22];
[b] Our results (this work);
[c] Reference [23].

The light-induced FSDP changes indicate the photoexpansion in g-As_2S_3 which is caused, as suggested by Tanaka [22], by an increase in structural randomness accompanying the widening of the interlayer distance in some places. Taking into account an agreement between the light and γ-ray excitation influence on the FSDP characteristics the same changes can take place in the case of γ-irradiation of g-As_2S_3. The radiation-induced changes in void-species nanostructure can be related to the creation of new nanovoids in the glass matrix after irradiation. This can plausibly be explained in the framework of coordination topological defect formation concept described in detail in [24,25].

According to the concept of coordination topological defect formation, radiation-induced structural transformations or chemical bond switching reactions in the glass network result in the formation of positively and negatively charged coordination topological defects (CTDs) as illustrated in Fig. 6 for the case of g-As_2S_3 [24, 25].

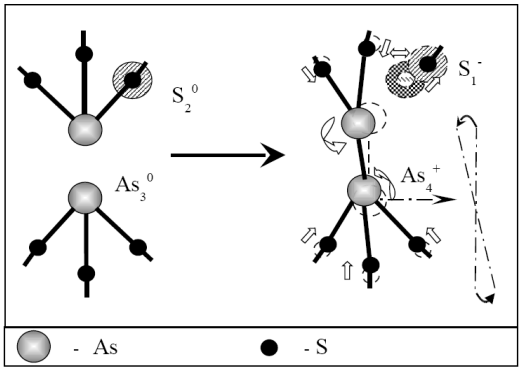

Fig. 6. Schematic illustration of radiation-induced covalent bond switching processes in g-As_2S_3 accompanied with formation of positively and negatively charged As_4^+ and S_1^- coordination topological defects (CTDs) [24, 25].

Two different processes can be realized within CTD formation. The first one is appearance of an additional free volume in the vicinity of negatively charged S_1^- CTD due to the lack of one covalent bond and its shift towards another directly-linked atom (crosshatched space in Fig.

6). In opposite, the second process corresponds to a decreasing of the free volume in the vicinity of positively charged As_4^+ CTD during formation of the new structural fragments with homopolar As-As covalent chemical bonds involving two arsenic and five sulphur atoms with reduced total volume owing to atomic displacements instead of two pyramidal structural units $AsS_{3/2}$. The creation of new nanovoids after irradiation can be caused by formation of negatively charged S_1^- CTDs. At the same time, the observed increasing in the average coordination near As atoms established by HEXRD and EXAFS experiments can reasonably be explained as a result of the radiation-induced formation of over-coordinated As_4^+ defects.

5. Conclusion

Atomic- and void-species nanostructures for the unmodified and γ-irradiated As_2S_3 glass are studied using conventional XRD, synchrotron-based HEXRD and EXAFS techniques. The experimental results obtained show that γ-induced structural modification of g-As_2S_3 leads to the significant changes in nanoscale atomic and void topology of the glass network. The decrease in packing factor of amorphous layers, increase in structural disordering, creation of new nanovoids, and increase of the coordination number and mean square deviation in bond length (the Debye-Waller factor) are the main radiation-induced features observed. The structural changes in γ-irradiated g-As_2S_3 are explained in terms of coordination topological defects.

Acknowledgments

This work was carried out within INTAS. T. K. gratefully acknowledges a grant by INTAS (Ref. Nr. 05-109-5323) for Young Scientist Fellowship and his staying in Chemnitz University of Technology (Germany) and Jan Dlugosz University in Czestochowa (Poland). T. K. and I. K. also acknowledge Deutsches Elektronen-Synchrotron DESY for support of the experiments performed at HASYLAB (Hamburg, Germany). Pal Jovari is acknowledged for his help with experimental data treatment.

References

[1] A. Feltz, Amorphous and Vitreous Inorganic Solids, Mir, Moscow, 1986.
[2] M. Popescu, Non-Crystalline Chalcogenides, Kluwer Academic Publishers, Dordrecht-Boston-London, 2000.
[3] A. K. Pikaev, Modern Radiation Chemistry: Main Principles, Experimental Technique and Methods, Nauka, Moskow (1985).
[4] I. A. Domoryad, B. T. Kolomijetz., Izv. AS SSSR. Neorgan. Mater. **7**, 1620 (1971).
[5] I. A. Domoryad, B. T. Kolomijetz, V. M. Lyubin, V. P. Shylo,, Izv. AS SSSR. Neorgan. Mater. **11**, 743 (1975).
[6] H. F. Poulsen, J. Neuefeind, H.-B. Neumann, J.R. Schneider, M.D. Zeidler, J. Non-Cryst. Solids **188**, 63 (1995).
[7] J. Krogh-Moe, Acta Cryst. **9**, 951 (1956).
[8] N. Norman, Acta Cryst. **10**, 370 (1957).
[9] D.T. Cromer, J.B. Mann, J. Chem. Phys. **47**, 1892 (1967).
[10] T.E. Faber, J.M. Ziman, Philos. Mag. **11**, 153 (1965).
[11] A. Guinier, X-ray Diffraction, Freeman, San Francisco, 1963.
[12] A. Lőrinczi, J. Optoelectron. Adv. Matter. **1**, 37 (1999).
[13] C.J. Brabec, Phys. Rev. B **44**, 13332 (1991).
[14] T.G. Fowler, S.R. Elliott, J. Non-Cryst. Solids **92**, 31 (1987).
[15] T.S. Kavetskyy, O.I. Shpotyuk, J. Optoelectron. Adv. Mater. **7**, 2267 (2005).
[16] S.R. Elliott, Phys. Rev. Lett. **67**, 711 (1991).
[17] S.R. Elliott, J. Non-Cryst. Solids **182**, 40 (1995).
[18] K.O. Jensen, P.S. Salmon, I.T. Penfold, P.G. Coleman, J. Non-Cryst. Solids **170**, 57 (1994).
[19] T. Kavetskyy, O. Shpotyuk, V. Boyko, J. Filipecki, M. Popescu, Bull. Lviv. Univ. Ser. Phys. **40**, 153 (2007).
[20] M. Popescu, J. Non-Cryst. Solids **35-36**, 549 (1980).
[21] S. Hosokawa, Y. Kawakita, W.-C. Pilgrim, F. Hensel, J. Non-Cryst. Solids **293-295**, 153 (2001).
[22] Ke. Tanaka, Phys. Rev. B **57**, 5163 (1998).
[23] A. Kolobov, H. Oyanagi, K. Tanaka, Ke. Tanaka, Phys. Rev. B **55**, 726 (1997).
[24] O. Shpotyuk, J. Filipecki, Free Volume in Vitreous Chalcogenide Semiconductors: Possibilities of Positron Annihilation Lifetime Study, WSP, Czestochowa, 2003.
[25] O. I. Shpotyuk, J. Filipecki, A. Kozdras, T.S. Kavetskyy, J. Non-Cryst. Solids **326-327**, 268 (2003).

*Corresponding author: shpotyuk@novas.lviv.ua